

Viscosity of Alternative Refrigerants R407C and R407E in the Vapor Phase from 298.15 to 423.15 K

C. Yokoyama,^{1,2} M. Takahashi,¹ and D. Tomida¹

Received June 18, 2004

This paper presents new measurements of the viscosity of gaseous R407C (23 mass% HFC-32, 25 mass% HFC-125, 52 mass% HFC-143a) and R407E (25 mass% HFC-32, 15 mass% HFC-125, 60 mass% HFC-143a). The measurements were carried out with an oscillating-disk viscometer of the Maxwell type at temperatures from 298.15 to 423.15 K. The densities of these two fluid mixtures were calculated with the equation-of-state model in REFPROP. The viscosity at normal pressures was analyzed with the extended law of corresponding states developed by Kestin et al., and the scaling parameters needed in the analysis were obtained from our previous studies for the viscosity of the binary mixtures consisting of HFC-32, HFC-125, and HFC-134a. The modified Enskog theory developed by Vesovic and Wakeham (V-W method) was applied to predict the viscosity for the ternary gaseous HFC mixtures under pressure. As for the calculation of pseudo-radial distribution functions in mixtures, a method based on the equation of state for hard-sphere fluid mixtures proposed by Carnahan-Starling was applied. It was found that the V-W method can predict the viscosity of R407C and R407E without any additional parameters for the ternary mixture.

KEY WORDS: corresponding states; Enskog theory; HFC-32; HFC-125; HFC-134a; mixture model; R407C; R407E; viscosity

1. INTRODUCTION

Potential alternatives for chlorofluorocarbons (CFCs) and hydrochlorofluorocarbons (HCFCs) include hydrofluorocarbons (HFCs), such as HFC-125 (pentafluoroethane), HFC-134a (1,1,1,2-tetrafluoroethane),

¹ Institute of Multidisciplinary Research for Advanced Materials (IMRAM), Tohoku University, Katahira 2-1-1, Sendai, 980-8577 Japan.

² To whom correspondence should be addressed. E-mail: chiaki@tagen.tohoku.ac.jp

HFC-143a (1,1,1-trifluoroethane), and HFC-32 (difluoromethane), and their binary and/or ternary mixtures.

Transport properties, such as viscosity and thermal conductivity, of the alternative refrigerants influence the economic feasibility of heat exchangers that can perform close to the theoretical efficiency of thermodynamic cycles using CFCs. Therefore, reliable prediction methods for the transport properties of mixed HFCs are essential to establish the process design methodology for a search of the optimum operating conditions of refrigeration systems using HFCs.

In our previous studies, we measured the gaseous viscosity of HFC-32, HFC-134a, HFC-143a, HFC-125 [1–4], HFC-125/134a [5], HFC-125/32 [6], and HFC-32/134a [7] systems. As part of a continuing study of the viscosity of dense fluid systems containing HFCs, measurements of the viscosity of gaseous R407C (23 mass% HFC-32, 25 mass% HFC-125, 52 mass% HFC-143a) and R407E (25 mass% HFC-32, 15 mass% HFC-125, 60 mass% HFC-143a) made at 298.15, 323.15, 348.15, 373.15, 398.15, and 423.15 K over a pressure range from 0.1 to near the vapor pressure under subcritical temperature conditions or up to 7.6 MPa under supercritical temperature conditions, are reported in this paper. The present viscosity values were compared with the experimental data for R407C measured by Nabizadeh and Mayinger [8].

Since the viscosities of the three pure HFCs and the three binary HFC mixtures related to R407C and R407E have been measured, we can check the predictive capability of a theoretical model with the use of the experimental viscosity values of R407C and R407E. The viscosity data at 0.1 MPa were compared with predictions by the extended law of corresponding states developed by Kestin et al. [9]. The viscosity data under pressure were analyzed with the extended Enskog theory developed by Vesovic and Wakeham [10]. The pseudo-radial distribution function for species *i* and *j* in the mixture needed in the viscosity prediction was calculated from the numerical method developed in our previous study [7] which is based on the equation-of-state model for hard-sphere fluid mixtures proposed by Carnahan and Starling [11].

2. EXPERIMENTAL

The viscosity was measured with an oscillating-disk viscometer of the Maxwell type. The experimental apparatus and procedures were the same as those described in previous studies [12–14]. The apparatus constant of the viscometer at the experimental temperature and pressure conditions was determined by considering the viscosity data of nitrogen taken from Stephan et al. [15] and the nitrogen gas density data from Jacobsen

et al. [16]. The apparatus constant varies slightly with temperature. On the other hand, under isothermal conditions, its variation with pressure is insignificant at the present experimental conditions. As for the gas density determination, we obtained density values for R407C and R407E from the equation-of-state model in REFPROP [17]. Temperature and pressure values have an uncertainty of 0.01 K and 0.5 kPa, respectively. The compositions of the sample mixtures were determined by weighing. The uncertainty of the composition determination was estimated to be less than 10^{-4} mole fraction. Based on the uncertainties of these properties, the uncertainty of the viscosity data is estimated to be within 0.5%.

The R407C and R407E samples were supplied by Asahi Glass Co. Ltd. The purities of both samples, certified by the suppliers, were approximately 99.9 mol%. The samples were used without any further purification. The sample gaseous mixtures were stored in a vessel which was thermostatted at about 423 K to prevent condensation.

3. RESULTS AND DISCUSSION

The experimental results for the viscosity of R407C and R407E are presented in Tables I and II, respectively. The viscosity values of R407C and R407E at 0.1 MPa are shown in Figs 1 and 2, respectively. In Fig. 1, the viscosity values reported by Nabizadeh and Mayinger are also plotted. As seen in Fig. 1, the present results for the viscosity of R407C at 0.1 MPa agree well with those of Nabizadeh and Mayinger [8]. The viscosity values of R407C under pressure are shown in Figs 3 and 4 and those of R407E in Figs 5 and 6. As can be seen for both fluids, the curves as a function of pressure intersect at higher temperatures (Figs 3 and 5), but the curves as a function of density do not (Figs 4 and 6). An initial negative density slope was observed for the viscosity at 298.15 and 323.15 K for both fluids. Almost the same behavior was observed for the pure constituent HFCs and their binary mixtures in our previous studies. In Figs 3 and 4, the viscosities of R407C measured by Nabizadeh and Mayinger [8] are also plotted. While their experimental temperatures are not exactly the same as those of this study, relatively large differences are observed for the pressure and density dependence of the viscosity isotherms. Their viscosity values at higher temperatures (323.15 and 333.1 K) show a larger density and/or pressure dependence. The source of relatively large discrepancies at high temperature and pressure conditions may be either in the density estimations or in the determination of the apparatus constant. Since large discrepancies can be observed in both Figs 3 and 4, the possible source of discrepancy may be in a method to evaluate the apparatus constant. As pointed out in our previous study [18], viscosity values determined by

Newell's theory [19] are very sensitive to the apparatus constant and are not as sensitive to the sample density.

The extended law of corresponding states for the transport properties developed by Kestin et al. [9] was applied to predict η_0 of R407C and R407E since all the scaling parameters have already been determined in our previous studies [1–7] and the values of the scaling parameters are listed in Table III. The calculated results are shown as the solid lines in Figs 1 and 2. It can be seen from these figures that the extended law of corresponding states represent the experimental viscosity η_0 quite well. The average absolute deviation between the experimental viscosity results and the calculated values is 0.18%, and the maximum deviation is 0.56% for R407C, and 0.41% and 1.03% , respectively, for R407E.

The viscosity under pressure is analyzed with the extended Enskog theory developed by Vesovic and Wakeham (V-W method) [10]. In the V-W method, we need the equations for the viscosity of pure constituent gases at 0.1 MPa and under pressure, and for mixture gases at 0.1 MPa. The viscosities at 0.1 MPa are obtained from the extended law

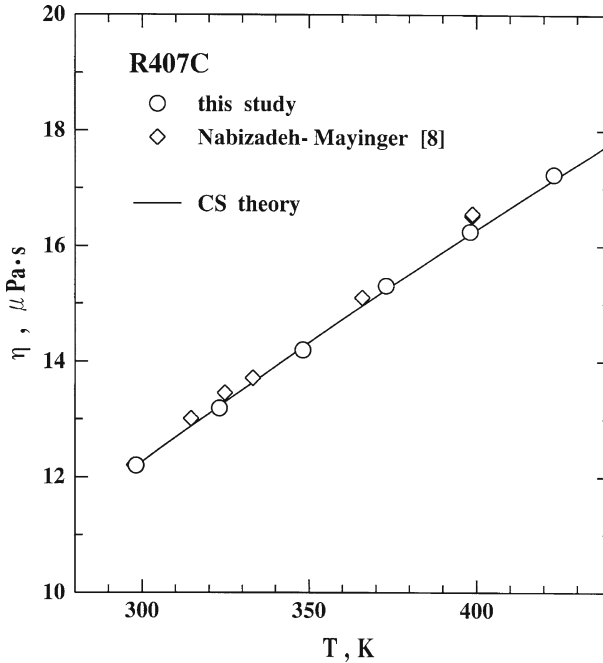


Fig. 1. Viscosity of R407C at 0.1 MPa.

Table I. Experimental Viscosity Values for R407C

T(K)	P(MPa)	$\rho(\text{kg} \cdot \text{m}^{-3})$	$\eta(\mu \text{ Pa} \cdot \text{s})$	T(K)	P(MPa)	$\rho(\text{kg} \cdot \text{m}^{-3})$	$\eta(\mu \text{ Pa} \cdot \text{s})$
298.15	0.1018	3.599	12.20	373.15	0.1003	2.807	15.24
	0.1024	3.620	12.19		0.1034	2.894	15.31
	0.2021	7.266	12.16		0.2911	8.261	15.40
	0.2890	10.55	12.12		0.5438	15.73	15.43
	0.3865	14.36	12.15		0.7805	23.00	15.46
	0.4666	17.61	12.10		1.027	30.88	15.47
	0.5689	21.92	12.07		1.273	39.08	15.52
	0.6638	26.09	12.11		1.525	47.88	15.65
	0.7614	30.59	12.05		1.814	58.51	15.76
	0.8643	35.60	12.08		2.112	70.16	15.91
323.15	0.9675	40.94	12.07	2.400	82.19	16.08	
	0.1020	3.313	13.21	2.678	94.63	16.33	
	0.1047	3.402	13.17	3.019	111.2	16.66	
	0.2206	7.271	13.15	3.306	126.6	16.95	
	0.3057	10.19	13.16	3.576	142.4	17.31	
	0.4063	13.72	13.15	3.955	167.6	18.00	
	0.5101	17.47	13.12	4.212	187.2	18.54	
	0.6026	20.91	13.15	4.397	203.1	19.05	
	0.7477	26.50	13.11	4.703	233.5	20.01	
	0.8970	32.53	13.15	4.937	261.7	21.07	
348.15	1.0249	37.96	13.21	5.115	287.3	22.13	
	1.1899	45.36	13.21	5.269	313.4	23.25	
	1.3401	52.54	13.27	5.1009	2.643	16.20	
	1.4937	60.46	13.31	0.1018	2.666	16.30	
	1.5947	66.00	13.36	0.2912	7.710	16.31	
	1.6899	71.52	13.41	0.4873	13.05	16.35	
	1.7839	77.31	13.48	0.6793	18.40	16.40	
	1.8833	83.84	13.54	0.9751	26.90	16.43	
	0.1001	3.009	14.16	1.267	35.61	16.50	
	0.1017	3.057	14.24	1.536	43.94	16.60	
0.2325	7.057	14.23	1.828	53.34	16.72		
0.3675	11.33	14.24	2.062	61.16	16.78		
0.5395	16.92	14.25	2.377	72.12	16.92		
0.7446	23.86	14.27	2.686	83.42	17.10		
0.9325	30.50	14.30	3.024	96.45	17.39		
1.123	37.54	14.29	3.408	112.2	17.70		
1.323	45.31	14.39	3.700	125.0	17.98		
1.521	53.43	14.47	4.014	139.5	18.32		
1.720	62.08	14.54	4.400	158.8	18.84		
1.904	70.58	14.65	4.654	172.4	19.26		
2.098	80.17	14.75	4.898	186.2	19.65		
2.256	88.52	14.92	5.194	204.1	20.21		
2.432	98.52	14.99	5.446	220.4	20.74		
2.587	108.0	15.18	5.643	234.0	21.26		
2.693	115.0	15.28	5.829	247.4	21.73		
2.875	128.1	15.50	6.027	262.5	22.30		

Table I. (continued)

T(K)	P(MPa)	$\rho(\text{kg} \cdot \text{m}^{-3})$	$\eta(\mu \text{ Pa} \cdot \text{s})$	T(K)	P(MPa)	$\rho(\text{kg} \cdot \text{m}^{-3})$	$\eta(\mu \text{ Pa} \cdot \text{s})$
398.15	6.252	280.7	22.99	423.15	3.488	102.2	18.53
	6.435	296.3	23.64		3.815	114.0	18.82
	6.591	310.3	24.31		4.220	129.3	19.18
423.15	0.1008	2.481	17.23	4.602	144.4	19.57	
	0.1016	2.501	17.25	4.950	158.8	19.98	
	0.2279	5.642	17.27	5.249	171.7	20.35	
	0.4055	10.12	17.26	5.527	184.2	20.75	
	0.7093	17.96	17.31	5.973	205.3	21.40	
	1.113	28.74	17.40	6.298	221.4	21.95	
	1.498	39.42	17.54	6.628	238.5	22.55	
	1.892	50.80	17.65	6.920	254.2	23.17	
	2.265	62.02	17.80	7.206	270.2	23.79	
	2.630	73.45	18.00	7.505	287.5	24.48	
3.115	89.37	18.30	7.690	298.4	25.08		

of corresponding states described above. The viscosity equations for pure constituent HFCs are obtained in our previous studies [1–3].

In the V-W method, the mean free path shortening factor, α_{ii} , and the switch-over density are obtained from the following relation,

$$(d\eta_i/d\rho)|_T = \eta_i/\rho \quad (1)$$

In the lower temperature range below 348.15 K, the switch-over densities at which Eq. (1) is valid are much higher than the maximum density of the present experimental conditions. Therefore, the Lee-Thodos (LT) viscosity correlation [20] was applied to Eq. (1). In the LT correlation, we used the extended law of corresponding states to calculate the viscosity at 0.1 MPa and treated the triple-point temperature as an adjustable parameter in order to improve the agreement between the experimental viscosity and correlated results. The optimum values of the triple-point temperature were 148.88 K for HFC-125, 180.98 K for HFC-134a, and 162.06 K for HFC-32.

As for the mixture viscosity calculations, the pseudo-radial distribution function χ_{ij} for species i and j in the mixture should be evaluated. In our previous study [6], we proposed a new method to calculate χ_{ij} from the exact theoretical equation for the radial distribution functions for the hard-sphere fluid mixture proposed by Carnahan and Starling [11]. As shown by Vesovic and Wakeham [10], the pseudo-radial distribution function for pure gases, χ_i , can be obtained from the pure-component viscosity by application of the hard-sphere expression for the viscosity of

Table II. Experimental Viscosity Values for R407E

T(K)	P(MPa)	$\rho(\text{kg} \cdot \text{m}^{-3})$	$\eta(\mu \text{ Pa} \cdot \text{s})$	T(K)	P(MPa)	$\rho(\text{kg} \cdot \text{m}^{-3})$	$\eta(\mu \text{ Pa} \cdot \text{s})$	
298.15	0.1020	3.505	12.14	373.15	0.1011	2.750	15.05	
	0.2000	6.989	12.08		0.1043	2.828	15.09	
	0.2954	10.50	12.07		0.2479	6.817	15.06	
	0.4896	18.06	12.06		0.4038	11.23	15.09	
	0.5939	22.39	11.98		0.6101	17.25	15.12	
	0.6940	26.75	12.03		0.8063	23.15	15.15	
	0.7913	31.20	12.01		1.017	29.72	15.18	
	0.8974	36.35	11.99		1.382	41.68	15.28	
	323.15	0.1029	3.249		13.04	1.576	48.39	15.35
		0.1025	3.236		13.11	1.782	55.79	15.41
0.2006		6.412	13.06	1.994	63.76	15.49		
0.2987		9.669	13.05	2.188	71.39	15.62		
0.3919		12.84	13.04	2.460	82.69	15.79		
0.5426		18.16	13.06	2.657	91.38	15.95		
0.6933		23.72	13.08	2.939	104.7	16.19		
0.8655		30.41	13.06	3.208	118.5	16.47		
0.9982		35.84	13.11	3.424	130.5	16.76		
1.160		42.86	13.13	3.645	143.8	17.09		
348.15	1.297	49.18	13.15	3.840	156.5	17.41		
	1.451	56.78	13.20	4.048	171.5	17.86		
	1.602	64.85	13.26	4.265	188.9	18.41		
	1.743	73.08	13.34	4.420	202.7	18.84		
	1.859	80.48	13.43	4.656	226.7	19.71		
	0.1016	2.968	14.09	4.826	247.0	20.54		
	0.1010	2.951	14.09	4.983	268.7	21.54		
	0.1973	5.817	14.10	5.082	284.4	22.36		
	0.3187	9.508	14.08	398.15	0.1008	2.566	16.07	
	0.4614	13.96	14.08		0.4215	10.93	16.09	
0.6215	19.12	14.09	0.7312		19.32	16.16		
0.7703	24.08	14.13	1.073		28.97	16.21		
0.9277	29.51	14.15	1.456		40.30	16.33		
1.075	34.78	14.16	1.776		50.24	16.40		
1.226	40.39	14.20	2.067		59.69	16.53		
1.375	46.16	14.26	2.381		70.37	16.65		
1.534	52.58	14.28	2.629		79.19	16.79		
1.691	59.24	14.33	2.935		90.59	17.03		
1.843	66.02	14.43	3.228	102.1	17.24			
1.987	72.78	14.51	3.437	110.7	17.46			
2.137	80.23	14.59	3.691	121.6	17.68			
2.277	87.60	14.70	3.941	132.9	17.95			
2.430	96.21	14.86	4.224	146.5	18.29			
2.597	106.4	15.00	4.424	156.6	18.58			
2.763	117.5	15.25	4.688	170.7	18.94			
2.971	133.4	15.58	4.895	182.5	19.31			
3.109	145.4	15.86	5.097	194.5	19.71			
3.205	154.9	16.11	5.256	204.5	20.06			

Table II. (continued)

T(K)	P(MPa)	$\rho(\text{kg} \cdot \text{m}^{-3})$	$\eta(\mu \text{ Pa} \cdot \text{s})$	T(K)	P(MPa)	$\rho(\text{kg} \cdot \text{m}^{-3})$	$\eta(\mu \text{ Pa} \cdot \text{s})$
398.15	5.507	221.1	20.62	423.15	2.826	77.66	18.03
	5.697	234.5	21.06		3.202	89.92	18.26
	5.813	243.0	21.47		3.468	98.93	18.54
	5.906	250.1	21.74		3.922	115.0	18.84
	5.998	257.3	22.01		4.302	129.2	19.14
423.15	0.1011	2.419	17.16	4.741	146.6	19.54	
	0.4217	10.24	17.20	17.16	4.978	156.3	
	0.7415	18.28	17.23	5.351	172.4	20.37	
	1.075	26.93	17.36	5.684	187.5	20.83	
	1.461	37.32	17.43	6.030	203.9	21.39	
	1.756	45.54	17.56	6.383	221.6	22.03	
	2.060	54.28	17.68	6.655	235.7	22.49	
	2.429	65.29	17.87	7.236	267.8	23.80	
				7.487	282.4	24.34	

Table III. Scaling Parameters of Extended Corresponding States for R407C and R407E

$i - j$	ϵ/k (K)	σ (nm)
HFC-134a–HFC-134a	278.31	0.50788
HFC-32–HFC-32	277.46	0.41530
HFC-125–HFC-125	235.85	0.52600
HFC-134a–HFC-32	303.63	0.46199
HFC-134a–HFC-125	240.16	0.52354
HFC-125–HFC-32	265.25	0.46024

a pure gas [Eqs (6) and (7) in Ref. 10]. We assumed that χ_i is equal to the Carnahan-Starling radial distribution function of pure hard-sphere fluid i as follows:

$$\chi_i = \frac{1}{(1 - \xi_3)} + \frac{3\xi_3^2}{2(1 - \xi_3)^2} + \frac{\xi_3^3}{2(1 - \xi_3)^3} \quad (2)$$

where ξ_3 is a reduced density defined by $(1/6)\pi\rho N_A d_i^3$, ρ is a molar density in $\text{mol} \cdot \text{cm}^{-3}$, N_A is Avogadro's number in mol^{-1} , and d_i is a hard-sphere diameter for species i in cm. Once the value of χ_i was obtained from the pure-component viscosity data, the d_i 's can be determined by solving Eq. (2). Equation (2) can be expressed as a cubic equation in ξ_3 , as shown in the following equation:

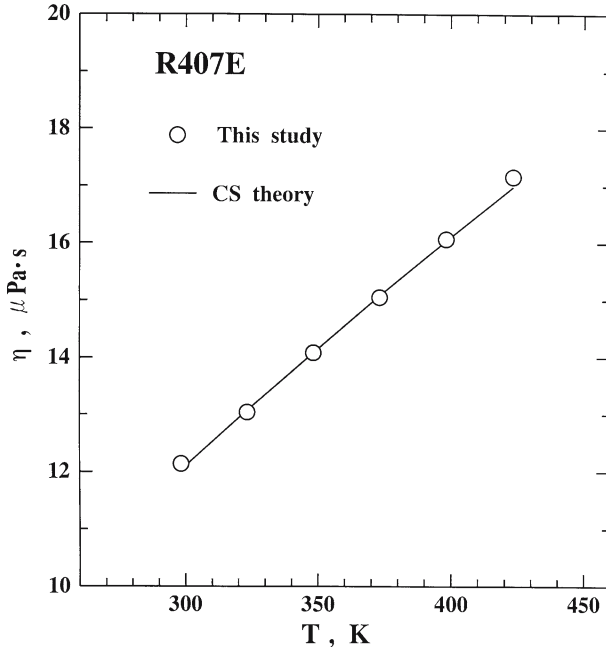


Fig. 2. Viscosity of R407E at 0.1 MPa.

$$\xi_3^3 - 3\xi_3^2 + \left(3 - \frac{1}{2\chi_i}\right)\xi_3 + \left(\frac{1}{\chi_i} - 1\right) = 0 \tag{3}$$

Since Eq. (3) has only a single real root under the present experimental conditions, the hard-sphere diameter value can be obtained from the following analytical equation:

$$\xi_3 = \frac{\pi}{6} \rho d_i^3 = \left(-\frac{n}{2} + \sqrt{D}\right)^{1/3} + \left(-\frac{n}{2} - \sqrt{D}\right)^{1/3} \tag{4}$$

where

$$D = \frac{n^2}{4} + \frac{m^3}{27} \tag{5}$$

$$n = \frac{27}{2\chi_i} \tag{6}$$

$$m = -\frac{1}{2\chi_i} \tag{7}$$

Once the hard-sphere diameters for every constituent species in the mixture are determined from Eqs (3)–(7), the pseudo-radial distribution

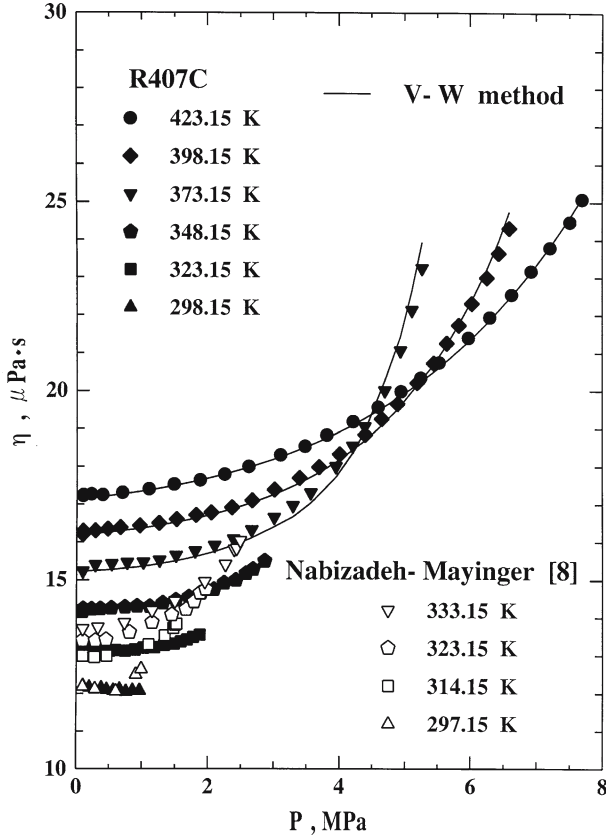


Fig. 3. Viscosity of R407C as a function of pressure.

functions for species *i* and *j* in the mixture were obtained from the Carnahan-Starling radial distribution function of hard-sphere mixtures [11]. In the case of a binary mixture of species *i* and *j*, the following equation holds:

$$x_{ij} = \frac{1}{(1 - \xi_3)} + \frac{3(d_i d_j) \xi_2}{(d_i + d_j)(1 - \xi_3)^2} + \frac{2(d_i d_j)^2 \xi_3^2}{(d_i + d_j)^2 (1 - \xi_3)^3} \tag{8}$$

The reduced density ξ_k ($k=2, 3$) for the binary mixture (*i*+*j*) is defined as follows:

$$\xi_k = \left(\frac{1}{6}\right) \pi \rho N_A (x_i d_i^k + x_j d_j^k) \tag{9}$$

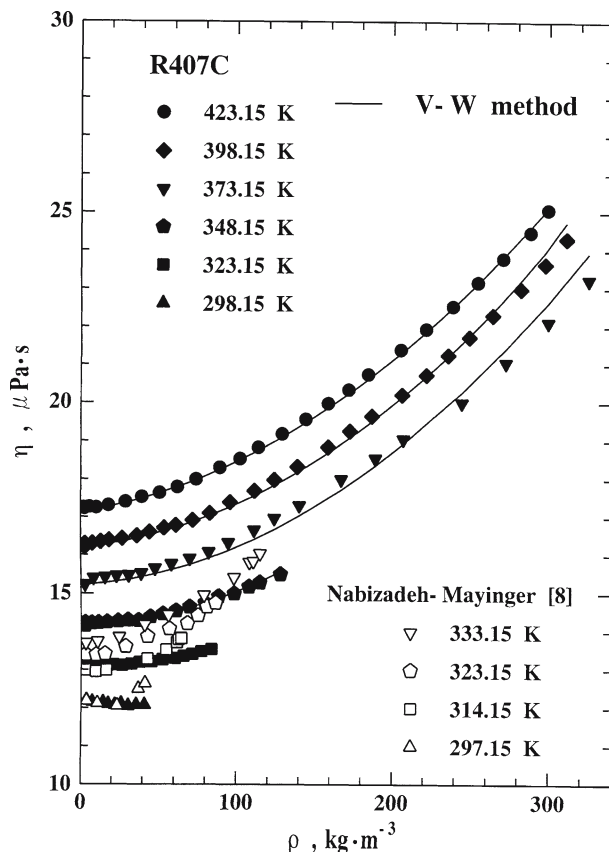


Fig. 4. Viscosity of R407C as a function of density.

where x_i is the mole fraction of species i . Since the Carnahan-Starling equation can give accurate results for the thermophysical properties for highly dense hard-sphere fluids, it is reasonable to consider that we can extrapolate $\chi_{ij}(\rho, T)$ to higher densities.

The solid lines in Figs 1 to 4 show the prediction results by the V-W method with the mixing rule shown in Eqs (2)–(9). Deviation plots based on the calculated values from the mixing rules of Eqs (2)–(9) are shown in Figs 7 and 8. The prediction results are listed in Table IV. It was found that the V-W method can represent the experimental viscosity of the HFC ternary mixture such as R407C and R407E quite well without any additional fitting parameters. This means that the V-W method is a predictive method for multicomponent HFC mixtures. The ability of the V-W

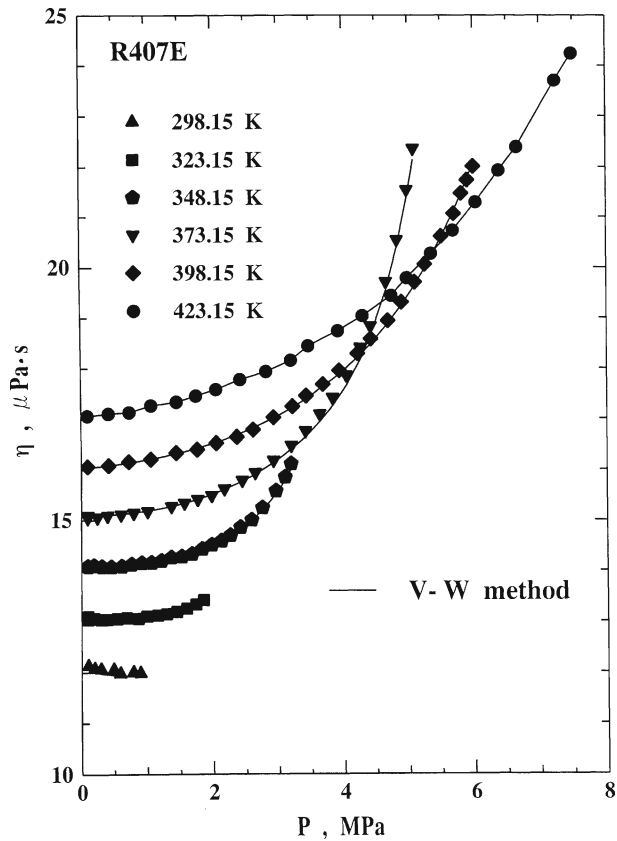


Fig. 5. Viscosity of R407E as a function of pressure.

Table IV. Prediction Results of the V-W Method for R407C and R407E

	n.d. ^a	BIAS (%) ^b	AAD (%) ^c	MAX (%) ^d
R407C	120	0.261	0.464	1.56
R407E	120	0.360	0.403	2.04

^an.d. : number of data.

^bBIAS (%) = $\sum 100(\eta_{\text{exp}} - \eta_{\text{cal}})/\eta$ n.d.

^cAAD (%) = $\sum 100|(\eta_{\text{exp}} - \eta_{\text{cal}})|/\eta_{\text{cal}}$ /n.d.

^dMAX (%) = maximum of $100|(\eta_{\text{exp}} - \eta_{\text{cal}})|/\eta_{\text{cal}}$

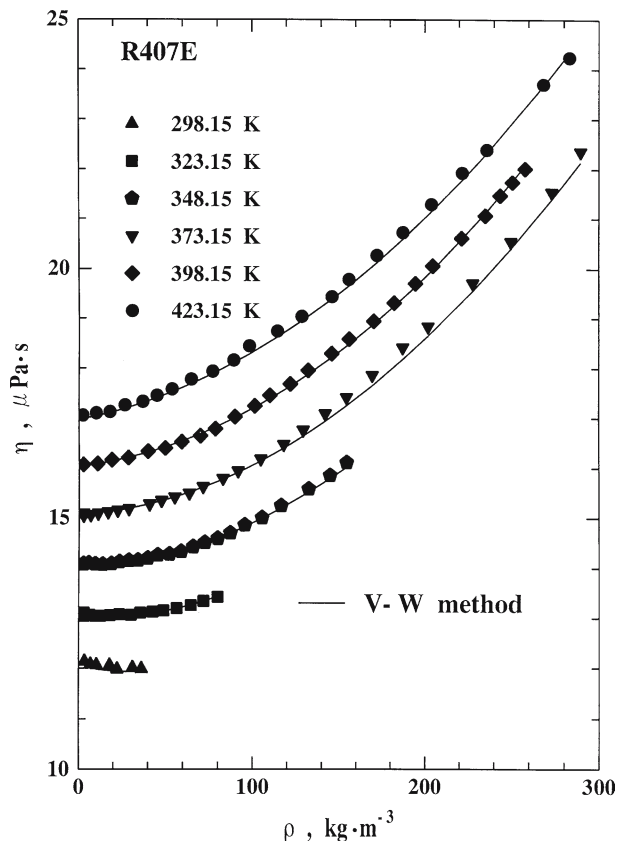


Fig. 6. Viscosity of R407E as a function of density.

method to represent the density and temperature dependence of the viscosity for the HFC ternary mixture may depend mainly on the viscosity correlations used for the pure constituent HFCs and also on the density correlations for the HFC mixture.

4. CONCLUSION

In this paper, we report experimental results of the gaseous viscosity for R407C and R407E. The present results for R407C were compared with the experimental data reported by Nabizadeh and Mayinger [8]. Their data deviate from the present results in the higher density (pressure) region. It was found that the viscosity at 0.1 MPa for the ternary mixtures can

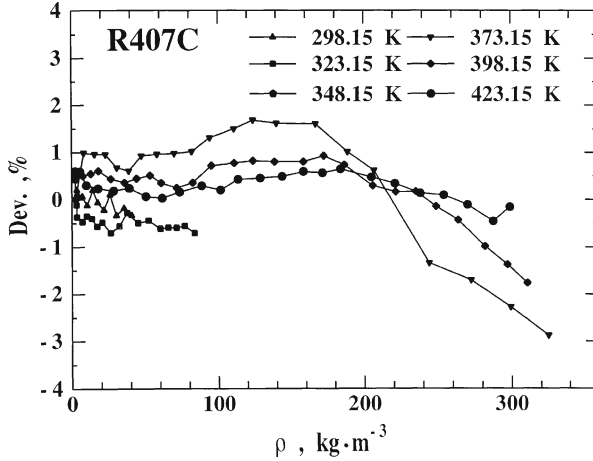


Fig. 7. Deviation plots for R407C. $\text{Dev. (\%)} = 100(\eta_{\text{exp}} - \eta_{\text{cal}})/\eta_{\text{cal}}$.

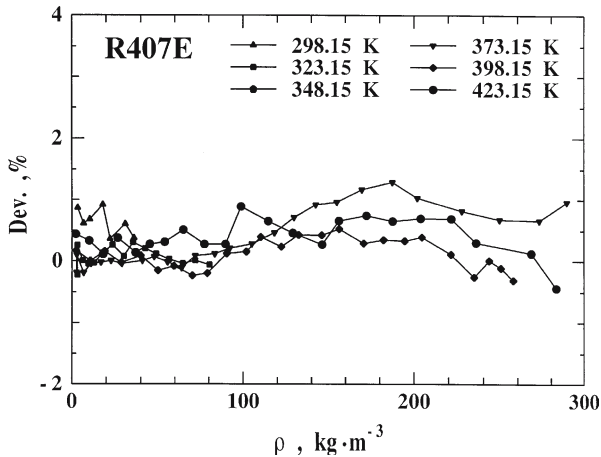


Fig. 8. Deviation plots for R407E. $\text{Dev. (\%)} = 100(\eta_{\text{exp}} - \eta_{\text{cal}})/\eta_{\text{cal}}$.

be represented with the extended law of corresponding states. The viscosity values of the gaseous mixtures under pressure can be predicted with the modified Enskog theory developed by Vesovic and Wakeham (V-W method) [10]. The pseudo-radial distribution functions needed for the viscosity predictions were determined from the method based on the exact equation for radial distribution functions for hard-sphere fluids developed by Carnahan and Starling [11]. It should be noted that the V-W method should be a reliable method for viscosity predictions for multicomponent

mixtures of HFCs under pressure, for the case when the viscosities of the pure HFCs under pressure and of the binary gaseous HFC mixtures under normal pressure are available and also when the density of gas mixtures under pressure can be predicted and/or correlated with high accuracy using an equation-of-state model such as that in REFPROP.

ACKNOWLEDGMENT

This study was supported from the research project entitled "Infrastructure development of thermophysical properties data for future industries" organized by the Japan Space Utilization Promotion Center (JSUP) and New Energy Industrial Technology Development Organization (NEDO), which is gratefully acknowledged.

REFERENCES

1. M. Takahashi, N. Shibasaki-Kitakawa, C. Yokoyama, and S. Takahashi, *J. Chem. Eng. Data* **40**:900 (1995)
2. N. Shibasaki-Kitakawa, M. Takahashi, and C. Yokoyama, *Int. J. Thermophys.* **19**:1285 (1998)
3. M. Takahashi, N. Shibasaki-Kitakawa, and C. Yokoyama, *Int. J. Thermophys.* **20**:435 (1999)
4. M. Takahashi, N. Shibasaki-Kitakawa, and C. Yokoyama, *Int. J. Thermophys.* **20**:445 (1999)
5. C. Yokoyama, T. Nishino, and M. Takahashi, *Fluid Phase Equilib.* **174**:231 (2000)
6. C. Yokoyama, T. Nishino, and M. Takahashi, *Int. J. Thermophys.* **22**:1329 (2001)
7. C. Yokoyama, T. Nishino, and M. Takahashi, *Int. J. Thermophys.* **25**:71 (2004)
8. H. Nabizadeh and F. Mayinger, *Int. J. Thermophys.* **20**:777 (1999)
9. J. Kestin, K. Knierim, E. A. Mason, B. Najafi, S. T. Ro, and M. Waldman, *J. Phys. Chem. Ref. Data* **13**:229 (1984)
10. V. Vesovic and W. A. Wakeham, *Int. J. Thermophys.* **10**:125 (1989)
11. N. F. Carnahan and K. E. Starling, *J. Chem. Phys.* **51**:635 (1969)
12. M. Takahashi, C. Yokoyama, and S. Takahashi, *J. Chem. Eng. Data* **33**:267 (1988)
13. M. Takahashi, C. Yokoyama, and S. Takahashi, *Trans. JAR* **6**:57(1989)
14. C. Yokoyama, M. Takahashi, and S. Takahashi, *Int. J. Thermophys.* **15**:603 (1994)
15. K. Stephan, R. Krauss, and A. Laesecke, *J. Phys. Chem. Ref. Data* **16**:993 (1987)
16. R. T. Jacobsen and R. T. Stewart, *J. Phys. Chem. Ref. Data* **2**:757 (1973)
17. NIST REFPROP Database, Version 6.01 (Nat. Inst. Stand. Technol., Boulder, Colorado, 1998)
18. C. Yokoyama and M. Takahashi, *Int. J. Thermophys.* **21**:695 (2000)
19. G. F. Newell, *ZAMP* **10**:160(1959)
20. H. Lee and G. Thodos, *Ind. Eng. Chem. Res.* **29**:1404 (1990)